

# The Application of FSI Techniques in Modeling of Realist Pulmonary Systems

Abdurrahim Bolukbasi, Hassan Athari, Dogan Ciloglu

**Abstract**—The modeling lung respiratory system that has complex anatomy and biophysics presents several challenges including tissue-driven flow patterns and wall motion. Also, the pulmonary lung system because of that they stretch and recoil with each breath, has not static walls and structures. The direct relationship between air flow and tissue motion in the lung structures naturally prefers an FSI simulation technique. Therefore, in order to toward the realistic simulation of pulmonary breathing mechanics the development of a coupled FSI computational model is an important step. A simple but physiologically relevant three-dimensional deep long geometry is designed and fluid-structure interaction (FSI) coupling technique is utilized for simulating the deformation of the lung parenchyma tissue that produces airflow fields. The real understanding of respiratory tissue system as a complex phenomenon have been investigated with respect to respiratory patterns, fluid dynamics and tissue viscoelasticity and tidal breathing period.

**Keywords**—Lung deformation and mechanics, tissue mechanics, viscoelasticity, fluid-structure interactions, ANSYS.

## I. INTRODUCTION

THE deformation of lung structure influences the airflow and suggests fluid-structure interaction problem with important actual modeling and clinical implications. For example, the construct of air fluid can lead to deteriorating lung function recognized as acute respiratory distress syndrome (ARDS) [1]. Also, during the ventilation of flow filled respiratory system, the micro-bubbles and interfaces of air-liquid in small pulmonary airways causes normal stresses and shear that may produce important cellular deformation. Although the stress problem that produce by the bubble induced has been investigated for rigid channels [2], [3], but the deformable cells may be critical for understanding the mechanisms of lung injury.

Normal respiration involves a process called negative pressure breathing. The lung air pressure equals atmospheric pressure as the lungs are at rest, and, therefore, the outward elastic recoil of the chest wall gets balanced by the inward elastic recoil of the lung walls. During each breath, the diaphragm moves down the inspiratory muscles contract the ribcage and produce the pressure gradient ( $\sim 2000 \text{ dyn/cm}^2$  or  $2 \text{ cmH}_2\text{O}$ ) by lung parenchyma [4]. This transmural pressure

expands the lung and establishes a sub-ambient pressure that produced by tissue stresses. Indeed, in the pulmonary system, tissue deformation drives the airflow field. Therefore, the direct relationship between tissue motion and airflow in the lung airways naturally suggests an FSI simulation technique. We note that although the FSI method has several desirable features but is computationally intensive. Our developed model produces airflow by utilizing an oscillatory pressure (1) to the tissue that is ignored by other research that prescribe fluid at simple definition [5]-[9].

$$P_{\text{load}} = \frac{\Delta P}{2} \left[ \sin \left( \frac{2\pi t}{\lambda_{\text{TB}}} - \frac{\pi}{2} \right) + 1 \right] \quad (1)$$

It is important that we determine a stress-free boundary condition rather than a prescribed flow profile at the duct inlet. As a result, tissue properties such as elasticity or viscosity can influence the amount of wall motion and alveolar flow patterns. Therefore, the development of a coupled FSI computational model is an important step toward the realistic simulation of alveolar-level breathing mechanics.

Inasmuch as tissue motion produces air flow in our developed models, it is significant to detect suitable physiological visco-elastic values for the tissue stiffness,  $E$ , tissue response time,  $\eta$  breathing frequencies,  $\lambda$ , and the value of the pressure used to the tissues correctly.

For this purpose, we extracted the baseline data which is provided by [10]. Table I shows the baseline values and the parameter ranges used in this study. We vary  $E$  to include a range of disease states in which the lung parenchyma is more or less stiff than normal tissue. We also vary the tissue viscosity,  $\eta$ , in a range that makes the ratio of stress relaxation time to breathing period vary from approximately 0.15 to 1.

TABLE I  
VALUE RANGES FOR SOLUTION PARAMETERS USED IN THE FINITE ELEMENT MODEL

Parameter	Baseline	Range
Tissue Viscosity (G/Cms)	$\eta = 30000$	$0 < \eta < 60000$
Tissue Elasticity (Dyn/Cm <sup>2</sup> )	$E = 40000$	$20000 < E < 50000$
Breathing Period (S)	$\lambda_{\text{TB}} = 5$	$5 \leq \lambda_{\text{TB}} \leq 15$

In this parameter variation study, the breathing period range includes  $\lambda_{\text{TB}} = 5 \text{ s}$ , or 12 breaths per minute, as well as slower breathing rates that may be of interest for drug delivery applications.

In the current study, we present a computational modeling of tissue-driven wall motion of the lung parenchyma tissue and the resulting oscillatory flow fields in an idealized model of the pulmonary system. In contrast to the models discussed

Abdurrahim Bolukbasi is with the Mechanical Engineering Department, Ataturk University, Erzurum, 25240, Turkey (e-mail: aboluk@atauni.edu.tr).

Hassan Athari is with the Department of Mechanical Engineering, Department, Ataturk University, Erzurum, 25240, Turkey (phone: +90-442-2314855; fax: +90-442-2360982; e-mail: Hassan.athari@atauni.edu.tr).

Dogan Ciloglu is with the Technical Vocational School of Higher Education, Ataturk University, Erzurum, 25240, Turkey (e-mail: dciloglu@atauni.edu.tr).

above, which use prescribed velocities and wall motions, the current FSI technique uses tissue motion to generate airflow within the alveolus. This approach allows us to study the influence of lung tissue mechanical properties on lung flow fields.

## II. FLUID-STRUCTURE INTERACTION TECHNIQUE

### A. Coupling Overview

This part starts by describing how the FSI coupling process works. The main features and capabilities are, then, discussed along with the current limitations. CFX solves Mass and Momentum equations in a single matrix (fully coupled) and iterations are required to converge the quantities transferred between the Transient structure and CFX solvers sequentially. As shown in Fig. 1 a transient 2-way FSI simulation has three levels of iterations:

- Field loop iterations stop when the field reaches its convergence target.
- Coupling loop iterations stop when the forces/ displacements reach their convergence targets or max number of Coupling Iterations.
- The transient loop-each /step moves forward in time, as in a standard CFD or FEA transient simulation.

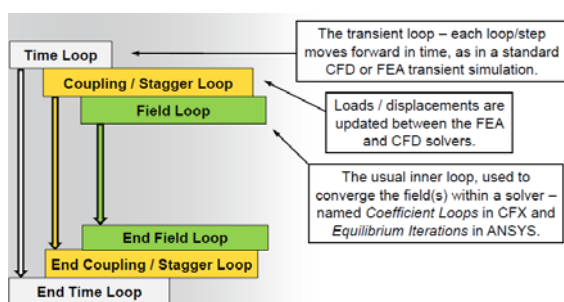


Fig. 1 Iterations of transient 2-way FSI simulation

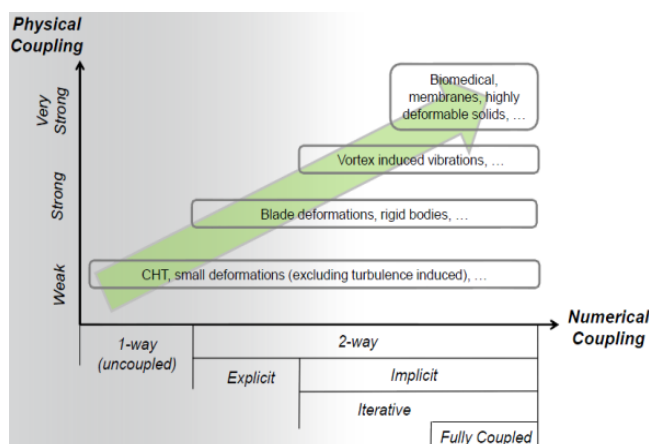


Fig. 2 The degree of physical coupling for different type FSI modeling approaches

### B. FSI Technique Categories

FSI Modeling Approaches can be categorized by the degree of physical coupling between the fluid and solid solution field (Fig. 2):

#### 1. One-Way Coupling Properties

- A converged solution is obtained for one field and then used as a boundary condition or external load for the second field.
- Suitable for weak physical coupling
- Easily done in Mechanical-CFX

#### 2. Two-Way Explicit Coupling Properties

- Can be done in Mechanical-CFX by using a single coupling iteration
- Solid solution is based on fluid field from the previous time step
- Generally requires much smaller time steps

#### 3. Two-Way Iteratively Implicit Coupling Properties

- Fluid and Solid equations solved separately
- Iterate within each time step to obtain an implicit solution ("stagger loops")
- Used in Mechanical- CFX

#### 4. Full Coupling Properties

- Fluid and Solid equations solved in a single monolithic matrix (Like Mass and Momentum in CFX, or coupled field elements in the Mechanical solver)
- Fields remain very tightly coupled
- However, very difficult to solve a monolithic fluid-structure matrix
- Not available with Mechanical -CFX coupling

### C. The Advantages of Using The CFX and Transient Structure (CT) in FSI technique

- The CT allows two-way fluid and structural coupling, including coupled field element solutions.
- The CT allows forces to be transferred from a pair of wall boundaries to a set of shell elements (2-to-1 mapping).
- Mesh smoothing options with CFX are more robust and have more control than Fluent.
- The CT allows mixed steady/transient couplings and allows restarts from steady-state to transient, neither of which is supported with SC.

### D. Standard Workbench Workflow for Two-Way FSI (Fig. 3)

- Drop a CFX system onto the Setup cell of a Transient Structural system.
- Geometry is shared by default.
- Fluid and structural meshes are created separately.
- CFX Solution cell controls the FSI simulation.
- Structural Solution not used for FSI, but can be used to check the structural model and create the FSI interface region where fluid forces will be received.

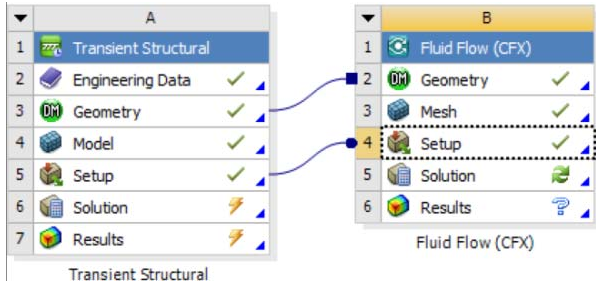


Fig. 3 The two-way FSI set up on Workbench

### E. Fluid-Structure Interaction Equations

We employ the (ANSYS) (FE) package to solve our FSI problem [11], [12]. The ANSYS solver employs a mixed discretization with an arbitrary Lagrangian–Eulerian (ALE) formulation. The deformable walls have a Lagrangian formulation, and the fluid domain has a Eulerian formulation. The fluid and solid solutions are coupled through continuity boundary conditions for displacement, traction, and velocity at the fluid-structure boundary. Fluid flow in the ANSYS model is governed by the incompressible form of the Navier–Stokes equations.

$$\rho \frac{\partial v_i}{\partial z_i} = 0 \quad i=1, 2, 3 \quad (2)$$

$$\rho \frac{\partial v_i}{\partial t} + \rho v_j \frac{\partial v_i}{\partial z_j} = -\rho \frac{\partial p}{\partial z_i} + \mu \frac{\partial^2 v_i}{\partial z_i \partial z_i} \quad (3)$$

where  $\rho$ ,  $\mu$ ,  $v$ ,  $t$  and  $p$  are density, viscosity, velocity vector, local vector and pressure of fluid respectively.

$$\frac{\partial \sigma_{ij}^s}{\partial z_i} = 0 \quad i=1, 2, 3 \quad (4)$$

$$\sigma_{ij}^s = \frac{E}{1+\nu} \epsilon_{ij} + \frac{\nu E}{(1+\nu)(1-2\nu)} \epsilon_{kk} \delta_{ij} \quad (5)$$

$$\epsilon_{ij} = \frac{1}{2} \left( \frac{\partial d_i}{\partial z_j} + \frac{\partial d_j}{\partial z_i} \right) \quad (6)$$

Similarly,  $\sigma_{ij}^s$ ,  $E$ ,  $\nu$ ,  $\epsilon^{ij}$  are stress tensor, elasticity modulus, Poisson's and tensile strength tensor respectively. The results will be made to the visco-elastic model by the help of Kelvin-Voigt visco-elastic model as shown in Fig. 4.

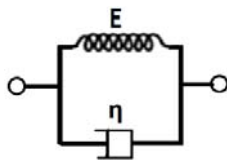


Fig. 4 The visco-elastic Kelvin-Voigt model

The Kelvin–Voigt model has both elasticity and viscosity properties simultaneously. Therefore the purely viscous damper and purely elastic spring can be connected in parallel form for representing the Kelvin–Voigt model.

$$\sigma_{\text{Total}} = \sigma_D + \sigma_S \quad (7)$$

$$\epsilon_{\text{Total}} = \epsilon_D = \epsilon_S \quad (8)$$

$$\sigma_{ij}^s = E \epsilon_{ij} + \eta \frac{\partial \epsilon_{ij}}{\partial t} \quad (9)$$

$$\epsilon_{ij} = \frac{1}{2} \left( \frac{\partial d_i}{\partial z_j} + \frac{\partial d_j}{\partial z_i} \right) \quad (10)$$

In (9)  $\eta$  is the viscosity. The boundary conditions at the interface regions between the two domains must be satisfied by coupling the fluid and structure domains at FSI modeling technique as shown below.

$$d_i^f = d_i^s \quad (11)$$

$$n_j \sigma_{ij}^s = n_j \sigma_{ij}^f \quad (12)$$

$$\sigma_{ij}^f = -p \sigma_{ij} + \mu \left( \frac{\partial v_i}{\partial z_j} + \frac{\partial v_j}{\partial z_i} \right) \quad (13)$$

$$n_j v_i = n_i \frac{\partial d_i^s}{\partial t} \quad (14)$$

In (9) the fluid and structure nodal displacements are shown by  $d_i^f$  and  $d_i^s$  respectively. Also,  $n_j$  is the normal interface vector,  $\sigma_{ij}$  is the Kronecker delta function. The fluid and solid stress tensors are shown by  $\sigma_{ij}^s$  and  $\sigma_{ij}$  respectively. The fluid velocity continuity condition in (14) needs that the structure and fluid domains have equal nodal velocities at the movable fluid–structure boundary.

We use an iterative solution scheme in ANSYS for computing the two-way coupling between the fluid and solid domain. For this purpose, we set up a pair of coupled systems which consisting of a Transient Structural system and a Fluid Flow (CFX) system for performing the two-way FSI analysis in ANSYS Workbench 16.

In this research, we utilize an independent discretization model of the fluid and structure domains. The FSI technique defines the interface between the structure domain in the Transient Structural system and fluid domain in the CFX system. Data of solid and fluid conditions is interchanged across this interface during the implementation of the simulation.

### F. The Airflow Modeling

The airflow field modeling was prepared by computational fluid dynamics (CFD) code using the ANSYS Workbench finite element solution algorithm. In this study, we use the laminar, incompressible and isothermal Navier–Stokes equations with the air specifications at 37°C for modeling the air flow conditions at the alveolar region.

## III. RESULTS AND DISCUSSION

The flow field that was computed on duct model has been showed for all generations 18–22 in Fig. 4. The flow field was represented by separation streamlines that computed by post processing on alveolar. The obtained flow fields have similar streamlines for all generations simulated. The flow in the center of the model, which has the greatest flow velocity, must speed up as it enters the outside of the lumen because of the created pressure gradient that represent the tissue motions. The

high-velocity region that positioned nearer the centerline of lumen segment at opening and outlet of the duct model was affected by pressure gradient significantly in low generations.

The achieved airflow streamlines can be compared by that seen in previous studies with low-Reynolds number flow and non-moving boundaries [6], [13].

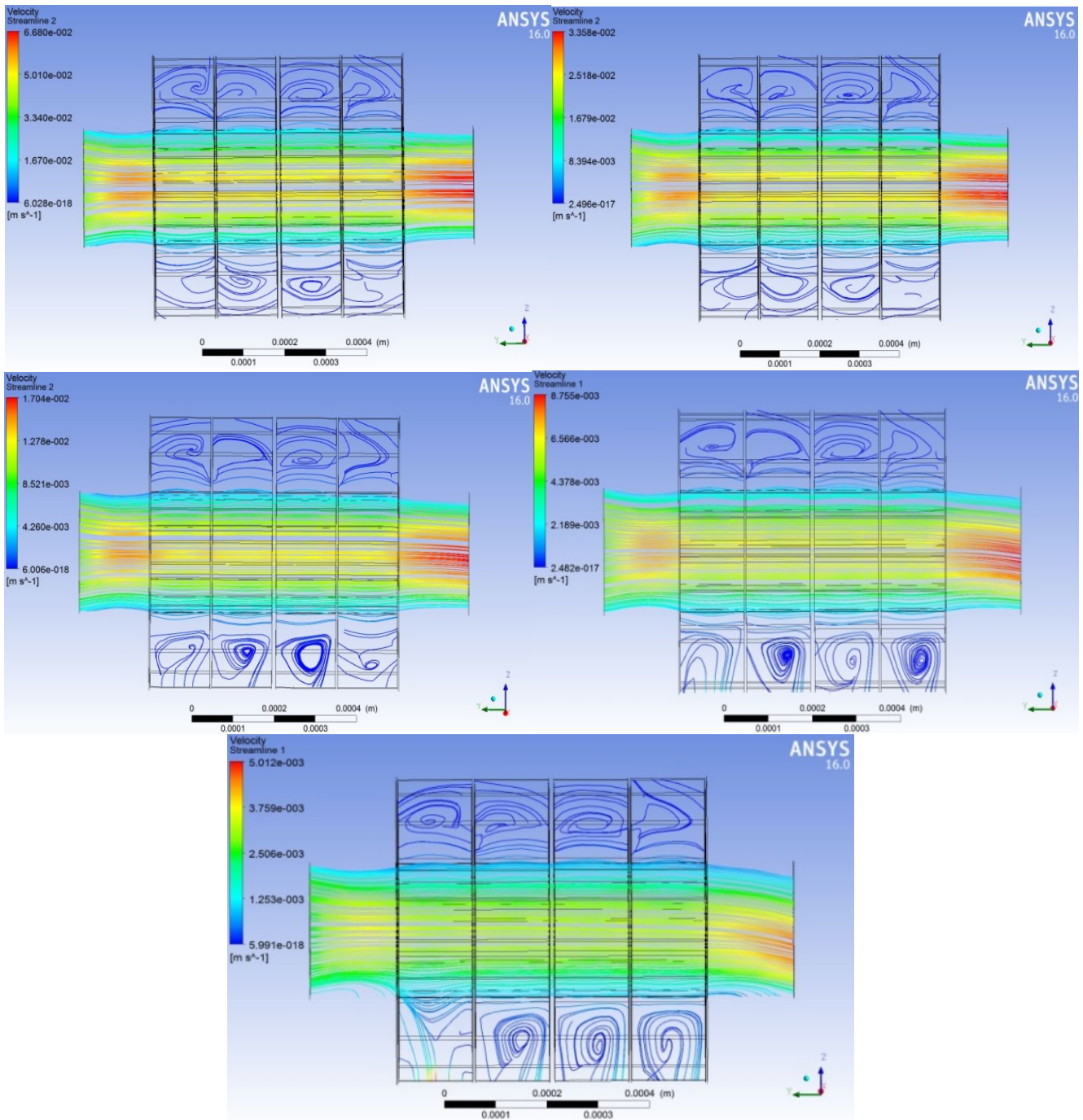


Fig. 5 The streamlines which colored by velocity magnitude in 18–22 generations with respected the gravity force acting on y-direction

According to Fig. 5 as the flow went down the lower generations (such as 22<sup>th</sup>), viscous forces dominate the flow because of low Reynolds number. Therefore, the velocity profile takes the parabolic shape. The velocity profile has been investigated on three separate plates for 22<sup>th</sup> generation that has been cleared in Fig. 6. As seen the profiles have a parabolic shape in plates which located at opening and outlet

of the model. Whereas the velocity profile of central plate has a heterogeneous shape because of pressure gradient effects.

The recirculation regions can be clearly observed in Fig. 5 where velocity vectors are displayed in alveolar cavities belonging to generations 18-22. A recirculation flow velocity that has approximately several times smaller than the mean lumen velocity was showed in each alveolus. It is clear that by

increasing generation number the recirculating regions have a relative circulate shape within alveoli geometry. The streamlines in our model, which had deformable walls, was

expected to analyze the faraway situations of proximal regions in the alveoli accurately.

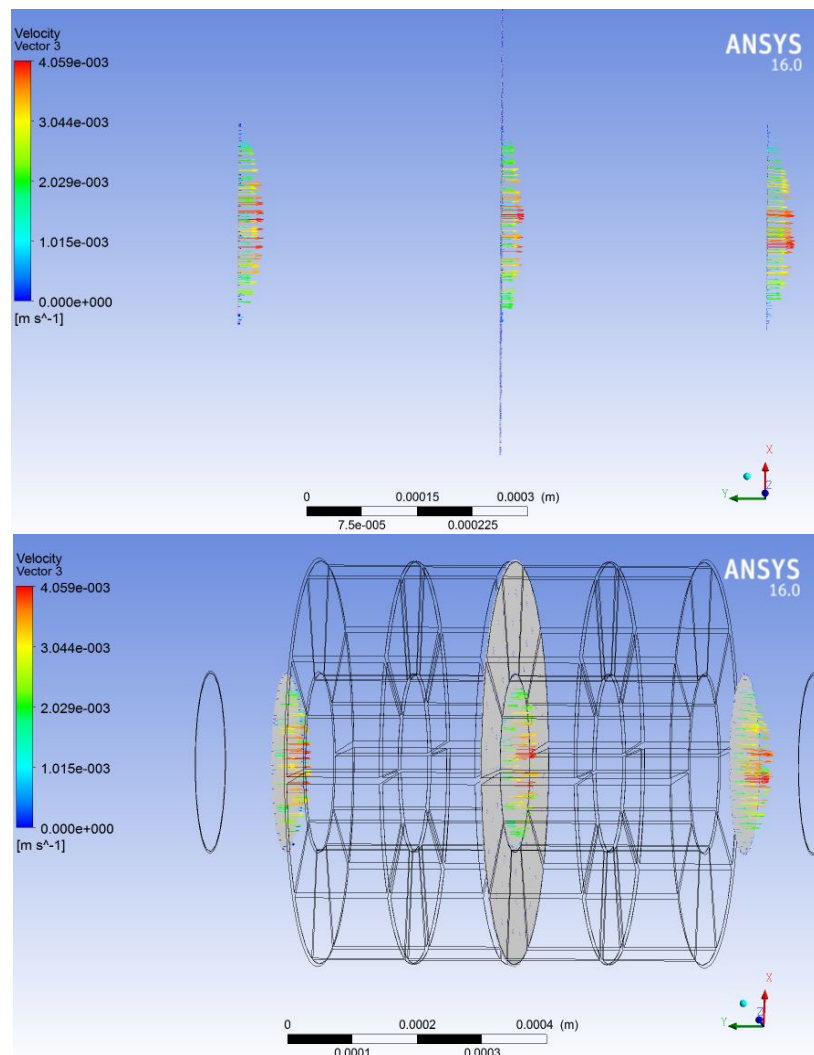


Fig. 6 The velocity profile at three separated planes that situated at known locations of model in 22th generation with respected the gravity force acting on z-direction

#### ACKNOWLEDGMENT

This research was supported by the BAP-2013/97 project of the Research Fund of Ataturk University.

#### REFERENCES

- [1] L.B. Ware, M.A. Matthay, "The acute respiratory distress syndrome," *New Eng J Med* 2000 vol.18, pp.1334-49.
- [2] J.D. Ricard, D. Dreyfuss and G. Saumon. "Ventilator-induced lung injury," *Eur Respir* 2003 vol.22, pp.42-48.
- [3] A.M. Jacob and D.P. Gaver, "An investigation of the influence of cell topography on epithelial mechanical stresses during pulmonary airway reopening," *Phys Fluids* 2005 vol.17, pp. 315-322.
- [4] M.G. Levitzky. "Pulmonary physiology," New York: McGraw-Hill 1991.
- [5] C. Darquenne, "A realistic two-dimensional model of aerosol transport and deposition in the alveolar zone of the human lung," *Journal of Aerosol Science*, 32, pp. 1161-1174, 2001.
- [6] C. Darquenne and G.K. Prisk, "Effect of gravitational sedimentation on simulated aerosol dispersion in the human acinus," *Journal of Aerosol Science* 2002 vol. 34, pp. 405-418.
- [7] S. Haber, J.P. Butler, H. Brenner, I. Emanuel and A. Tsuda, "Shear flow over a self-similar expanding pulmonary alveolus during rhythmical breathing," *Journal of Fluid Mechanics* 2000 vol. 405, pp. 243-268.
- [8] F.S. Henry, J.P. Butler and A. Tsuda, "Kinematically irreversible acinar flow: a departure from classical dispersive aerosol transport theories," *Journal of Applied Physiology* 2002 vol. 92, pp. 835-845.
- [9] A. Tsuda, J.P. Butler and J.J. Fredberg, "Effects of alveolated duct structure on aerosol kinetics I. Diffusional deposition in the absence of gravity," *Journal of Applied Physiology* 1994 vol. 76, pp. 2497-2509.
- [10] F.G. Hoppin, J.C. Stothert, I.A. Greaves, Y-L. Lai and J. Hildebrandt, "Lung recoil: elastic and rheological properties," In: A. Fishman, P. T. Macklem, J. Mead, & S. R. Geiger (Eds.), *Handbook of physiology*, III, mechanics of breathing, part 1 1986 pp. 195-215.
- [11] K-J. Bathe, H. Zhang and S. Ji, "Finite element analysis of fluid flows fully coupled with structural interactions," *Comput Struct* 1999 vol. 72, pp. 1-16.

- [12] K-J. Bathe and H. Zhang, "Finite element developments for general flows with structural interactions," *Int J Numer Met Eng* 2004 vol. 60, pp. 213–32.
- [13] L. Harrington, G. Kim Prisk and C. Darquenne, "Importance of the bifurcation zone and branch orientation in simulated aerosol deposition in the alveolar zone of the human lung," *J Aerosol Sci* 2006 vol. 37, pp.37–62.

**Abdurrahim Bolukbasi** is a faculty member of the Mechanical Engineering Department in Ataturk University, Erzurum, Turkey. He received his Ph.D. in 1997 on film boiling heat transfer. His remain research interests are boiling heat transfer, nanofluid heat transfer, CFD and numerical heat transfer. He has authored 23 conference and journal publications.

**Hassan Athari** is a doctoral student at Mechanical Engineering Department Ataturk University, Erzurum, Turkey. He completed his undergraduate education at Tabriz University, Tabriz, Iran. At Master Degree, he studied energy and exergy analysis of gas power plants. His M.S. thesis was accepted in 2009 and he began doctoral education after this. He is interested in FSI numerical techniques and CFD methods. He has authored 13 conference and journal publications.

**Dogan Ciloglu** is an assistant professor in the Technical Vocational School of Higher Education, Ataturk University, Erzurum, Turkey. He obtained his bachelor's degree in 2000 from Ataturk University. He experimented on pool film boiling around vertical cylinders for his master's thesis and received his M.S. in 2004. His doctoral research was focused on pool boiling heat transfer in nanofluids. He received his Ph.D. from Ataturk University in 2011. He is currently working on pool boiling heat transfer in nanofluids.